Mechanics and Mechanical Engineering
Vol. 20, No. 3 (2016) 309–321

Numerical Simulation of Axially Compressed Cylindrical Shells with Circular Cutouts

Olga Lykhachova
Department of Structural Mechanics and Strength of Materials
Prydniprovs'ka State Academy of Civil Engineering and Architecture
Chernyshevskogo 24a, 49600 Dnipropetrovs'k, Ukraine
lykhachova.olga@gmail.com

Received (10 June 2016)
Revised (20 June 2016)
Accepted (10 August 2016)

The present paper deals with FEM modelling of Tennyson's famous experiment: the buckling problem of axially compressed elastic cylindrical shells with small single circular cutouts. It is completed using ANSYS software package in geometrically linear and nonlinear formulations for three different loading schemes. Two of the loading schemes provide an upper and lower bounds for buckling loads. The third loading scheme corresponds to the experiment and gives an excellent agreement of numerical results with the experimental data. The influence of shell thickness on buckling load is studied in addition to common non–dimensional geometrical shell parameter. Decrease of a shell thickness about two times leads to decrease of buckling load parameter about 7 % in the studied range of cutouts. The efficiency of ANSYS software is proved for the buckling design of shells with highly non–homogeneous stress strain state.

Keywords: cylindrical shell, circular cutout, axial compression, loading scheme, buckling, numerical simulation.

1. Introduction

The buckling problem of axially compressed cylindrical shell with one circular cutout belongs to the set of typical and rather significant stability problems of shells with non-homogeneous stress strain state. A great number of researches (experimental, analytical and numerical) deal with the study of stability of shells with cutouts. The problem of buckling load calculation for cylindrical shells with cutouts became a particular one in 1947 after the studies made by Lur'e [1] and devoted to the analysis of the stress concentration around the circular openings. Early researches by Tennyson [2, 3] that included experimental results of the buckling problem of axially compressed elastic shells with a small circular cutout were one of the pioneer investigations. The first theoretical research performed by Van Dyke [4] provided a very good agreement with the experimental data [2]. Detailed information on the

initial stage of the stability investigation of shells with openings is presented in the reviews of Preobrazhenskii [5–6], Grigolyuk and Fil'shinskii [7], Guz and Ashmarin [8], Simitses [9], Teng [10], Song [11], Elishakoff [12].

The monograph [13] by Obodan, Lebedev, Gromov discussed the buckling problem of shells with large cutouts subjected essentially to external pressure as well as to axial compression. Stability of short reinforced and smooth shells with singular damages was studied by Kwok [14].

Researches [15] performed by Dzyuba, Prokopalo, Dzyuba Jr. generalised the experimental data of numerous tests of shells with openings of various shapes and numbers under different types of loading: axial compression, bending, torsion, and some their combinations.

We should mention the set of studies [16–18] of stability of composite cylindrical shells which were carried out by the scientists of NASA with the participation of Hilburger last two decades. The researches included experimental and numerical results for the shells with reinforced and unreinforced openings. The influence of geometrical imperfections, effect of delamination and non-uniform loading provoked by imperfect edges of a shell were estimated. There was also another early NASA work [19] by Starnes Jr. which comprised results of experimental and analytical investigations of the effect of a circular hole on the buckling of thin copper and Mylar cylinders. The simplified analytical Rayleigh-Ritz type approximation presented in [19] predicted the sharp reduction in buckling strength indicated by the experimental data only at low values of the hole parameter.

The related researches [20, 21] are associated with an intensive implementation of FEM program codes. These papers contained results of original experiments, as well as results of numerical simulations of the stability problem of the shells with single transversal cuts [21] and with single or several cutouts [20]. Among variable parameters considered in [20], there were different shapes (rectangular or circular) of openings, their locations and sizes in the circumferential and longitudinal directions. Besides, two non-classical types of kinematic loading conditions (loading schemes 2 and 4 according to the classification [22]) and the effect of real initial imperfections on the shell bearing capacity were studied. One of the most important results obtained by authors was an estimation of the coupling effect between initial geometrical imperfections and openings on the buckling loads. The study [21] confirms this result in the case of another non–classical boundary conditions the force loading scheme 1 (see Fig. 1) for the shells with imperfections similar to the first eigenmode found in preliminary linear buckling analyses.

Nowadays there is a stable trend to predict reliable buckling load by studying real behaviour of the structures with initial perturbations such as geometrical imperfections, discontinuities, external impacts, etc. We would like to attract attention to another factor that is very significant in the case of shell buckling problems with highly non–homogeneous stress strain state. This factor is connected with particularities of load application named loading schemes which can deeply affect magnitudes of main buckling parameters and change nonlinear behaviour of the shells. The work [22] demonstrates a significant spreading of buckling loads depending on loading conditions classified to five different loading schemes (see Fig. 1). These schemes take into account the type of loading (force N loading – schemes 1, 3, 5 or displacement ΔZ loading – schemes 2, 4) and three conditions

of applying an axial compression (with edge plane rotation – schemes 1, 2; with parallel edge displacement – schemes 3, 4; with out-of-plane edge displacements – scheme 5). The last scheme is classical one with uniform distribution of stresses in circumferential direction at the edge of the shell. Most theoretical solutions obtained using this boundary condition. However, in the practice and experiments it is not realised. The force (or displacement) is applied to the shell through a rigid element. The difference between all load conditions is significantly increasing in the case of non–homogeneous and nonlinear stress-strain states of the shells.

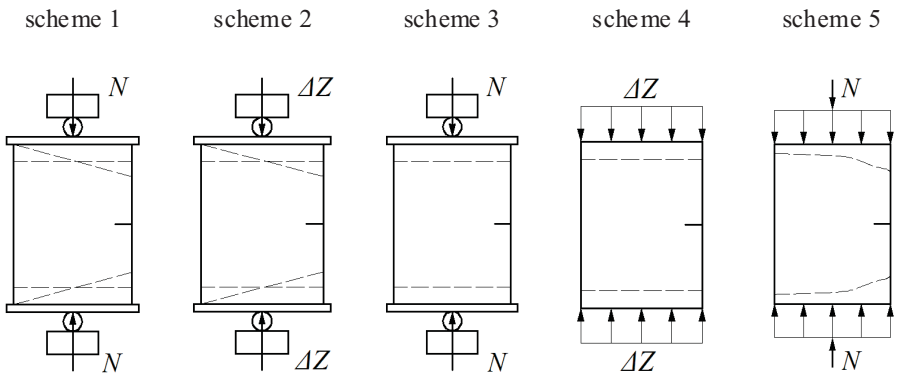

Figure 1 Loading schemes (in buckling moment)

The influence of shell thickness on buckling load parameters is not enough studied as well. Lekkerkerker's parameter $\mu = \frac{1}{2}\sqrt[4]{12\,(1-\nu^2)}\sqrt{a^2/Rh}$ is usually used to compare results of experiments and calculations. Here, R and h shell radius and its thickness, ν – Poison's ratio, a – cutout radius. However, experiments [19] show that for the same values of parameter μ the buckling load parameters are slightly lower if the shell is thinner. It is not clear if this is caused by sensitivity of the thinner shells to geometrical imperfections or the parameter μ should be adjusted to describe dependence on shell thickness.

The aim of the present research is the follows: testing simulations by ANSYS software package in case of non–homogeneous and nonlinear stress states of the shells; studying the influence of loading schemes and shell thickness on the value of buckling load.

In order to achieve these goals, a numerical modelling of well-known experiments of Tennyson [2] has been performed within ANSYS software. The advantage of this experiment is the very high quality of tested specimens. It allowed to obtain critical loads close to the classical value of axial compression, and to avoid the influence of usually unknown initial imperfections.

In the remainder, we will describe the methodology of the numerical simulation (Section 2). Obtained numerical solutions will be compared with experimental results and discussed in Section 3. The influence of loading conditions and shell thickness on buckling loads has been analysed in this section. The conclusion is derived in the last Section 4.

2. Methodology of the numerical research

The numerical simulation of the buckling tests [2] has been realised by means of the FE procedure implemented in ANSYS software. Three-dimensional FE models of the shells with real mechanical and geometrical characteristics: radius $R = 140$ mm, thickness $h = 0.48$ mm, $(R/h = 292)$, length $L = 560$ mm, $(L/R = 4.0)$ are considered. Elastic constants of isotropic photoelastic material are: modulus of elasticity $E = 2.82$ GPa, Poisson's ratio $\nu = 0.4$. Circular cutouts are located in the middle section of the shell length. The radius of cutouts varies as $a = 0$, 5.82, 8.32, 10.23, 10.7, 15.8, 20.9, 23.4 mm $(a/R = 0 \div 0.167)$ and corresponds to angular sizes $r = 0$, 2.38, 3.41, 4.19, 4.38, 6.47, 8.55, 9.58 degrees.

The numerical simulations of the experiment [2] have to satisfy all test conditions. Specimens [2] were loaded by screw with controlled displacements and with possible edge plane rotation (the scheme 2, see Fig. 1). Thus in the numerical models, the kinematic loading is realised as axial displacements ΔZ of the middle points C of the external surfaces of the rigid disks. An axial compressive force is calculated as a reaction N caused by the displacements ΔZ. Besides the scheme 2, two classical loading schemes are studied in this investigation: kinematical scheme 4 and force scheme 5 (see Fig. 1). In these two schemes, an axial compression is realised by uniformly distributed displacements (scheme 4) or by uniformly distributed forces (scheme 5) along the edges (in the circumferential direction) of a shell.

For the scheme 2, numerical models contain shell models themselves and also two rigid cylindrical disks of diameter equals to 140 mm and of height equals to 3 mm; while for the schemes 4 and 5, rigid disks are absent. The material of rigid disks is isotropic and elastic with characteristics $E = 2{\cdot}10^{15}$ Pa and $\nu = 0.3$. Note that according to the test conditions, it is allowed free rotations of the disks while loading. The FE mesh of the shell and rigid disks is created by standard elements SHELL181 and SOLID185 respectively from the standard ANSYS element library. First, shells are meshed with regular square elements; then the meshes are refined near the cutouts. Finally, an arbitrary FE mesh is created for the volumes of rigid disks (see Fig. 2b). The total number of elements varies between 45000 and 46000, including shell FEs – from 24700 to 26000 depending on the cutout size.

Boundary conditions of the scheme 2 include restrained radial and tangent displacements of the external edges of rigid disks. For the schemes 4 and 5, radial and tangent displacements are limited on the top and bottom edge of a shell. Besides, rotations of upper and lower shell edges are restricted for all considered schemes; and the shell is fixed in the longitudinal direction in the middle section of its length.

For all generated FE models it has been performed two analyses: 1) geometrically linear buckling analysis for the determination of eigenvalues and eigenmodes; 2) geometrically nonlinear stress strain state analysis for calculation of limit loads, longitudinal and transversal deformations. Nonlinear analysis is based on Newton-Raphson method [23] for kinematic schemes 2, 4 and on Arc–length method for the scheme 5.

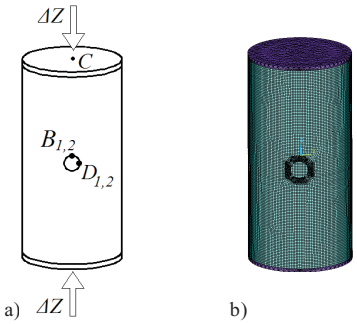

Figure 2 Loading scheme of a shell with one cutout (a) and finite element model (b)

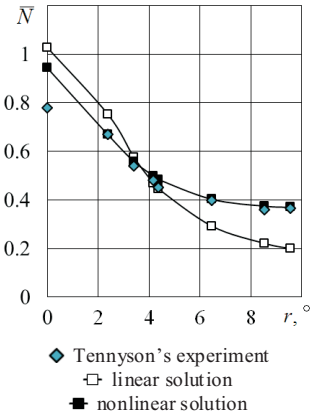

Figure 3 Dependences of relative experimental and numerical buckling loads on cutout r for the scheme 2

3. Numerical results and discussion

3.1. *Tennyson's experiments*

Fig. 3 represents the comparison of numerical simulation results for the scheme 2 with the experimental data [2] as dependences of dimensionless buckling loads $\overline{N} = N/N^{cl}$ ($N^{cl} = 2\pi Eh^2 \Big/ \sqrt{3(1-\nu^2)}$ – the classical critical axial compressive load for an isotropic cylindrical shell) on the cutout size r. Here, dark rhombs correspond to the experimental data, white squares – to critical loads of linear buckling analyses, black squares – to limit loads of geometrically nonlinear analyses.

The analysis of these dependences shows that the nonlinear solution completely coincides with the experimental data. Results of the linear buckling solution for the shell with small cutouts ($r < 4^o$) are higher than results of the geometrically nonlinear solution. For the shells with $r > 4^o$ the inversion of these two loads is observed. In the considered range of r the difference of linear and nonlinear analyses varies within $(0.017 \div 0.170)$ $\overline{N}$, and the biggest deviation occurs for the shell with $r = 9.58^o$.

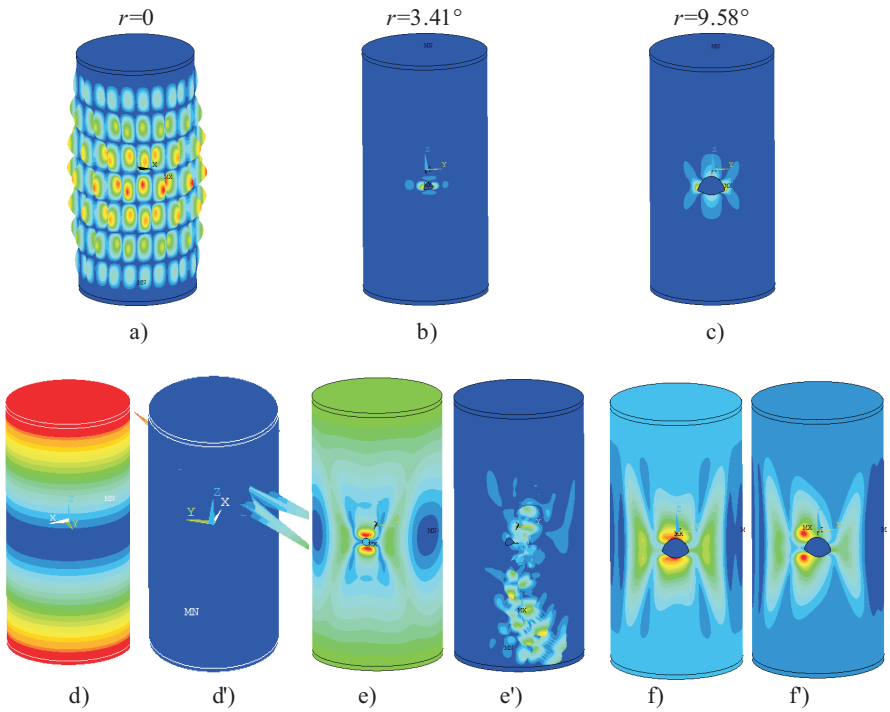

Figure 4 Buckling modes of linear analyses (a–c); pre–buckling (d–f) and post-buckling (d'–f') nonlinear deformations for the shells with r = 0, 3.41^o and 9.58^o

In case of nonlinear analysis we obtained a very good agreement between calculated and experimental data. The difference between the nonlinear solution and experimental data reaches its maximal value for a perfect shell ($r = 0$) and is equal to $0.165\ \overline{N}$, and for the rest cutouts ($r > 0$) these difference doesn't exceed $0.033\overline{N}$.

An effectiveness of the numerical approach performed in ANSYS software for shells with cutouts is also proved by matching of numerical buckling modes with the experimental buckling modes described in the paper [2].

Fig. 4a–c demonstrates characteristic buckling modes of shells with one cutout, obtained in linear buckling analyses. Here, a global bending deformation occurs in the case of perfect shell without any cutout. But for the rest range of studied shells, the buckling is local and mostly located near the cutouts.

In Fig. 4d–f, there are pictures of nonlinear pre–buckling modes (placed in boxes), which correspond to limit loads presented in Fig. 3. In Fig. 4d'–f' there are pictures of nonlinear post–buckling modes of shells with $r = 0$, 3.41^o and 9.58^o. It should be mentioned that in the geometrically nonlinear analysis, as well in the experiment [2], there were detected no one local buckling mode for the shells with $r \leq 4.38^o$. Note that for the shells with very small cutouts post-buckling modes are distributed on the shell surface (Fig. 4d'–e'). However, an increase of cutout size (see nonlinear buckling mode for $r = 9.58^o$, Fig. 4f') leads to the appearance of local post–buckling modes with two dents corresponding to the shell behaviour observed in the experiment.

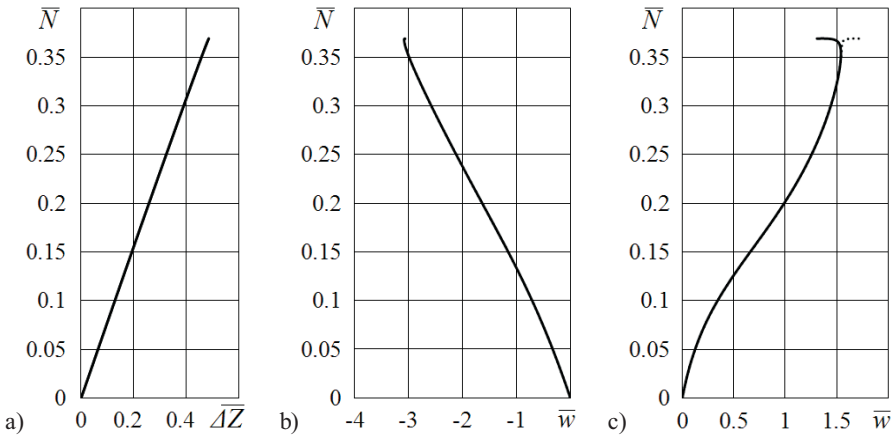

Figure 5 Deformation of the shell with cutout r=9.58^o

Typical curves in Fig. 5 illustrate the behaviour of the shell with cutout $r = 9.58^o$. These curves show dependences of relative compressive load on relative displacements of some points (see Fig. 2a): longitudinal displacement $\overline{\Delta Z} = \Delta Z/h$ of points $C_{1,2}$ (Fig. 5a: middle points of external surfaces of rigid disks); radial displacements $\overline{w} = w/h$ of points $B_{1,2}$ (Fig. 5b; points are situated on the boards of cutouts along

the generatrix) and points $D_{1,2}$ (Fig. 5c; points are situated on the boards of cutouts in the middle section of the shell). Here, the shortening $2\overline{\Delta Z}$ of the shell before the buckling is equal to about shell thickness. Corresponding relative radial displacements of points $B_{1,2}$ are symmetric and equal about $3h$. At the same time, relative radial displacements of points $D_{1,2}$ are non-symmetric and equal to $1.7h$.

3.2. *Comparisons of different loading schemes*

As we can notice, real loading conditions in the experiment [2] were different from classical axial compression. Classical loading is realised with uniformly distributed forces or displacements along the edges of a shell, rigid disks are absent. Compression with uniform forces (scheme 5) corresponds to the weakest boundary condition, which provides the lowest level of buckling loads according to the classification [22]. An axial compression with uniform displacements (scheme 4) is the most rigid boundary condition and corresponds to the highest level of buckling loads. This fact is illustrated by Fig. 6a–b. Here, white symbols correspond to linear solutions (Fig. 6a), and black symbols represent geometrically nonlinear solutions (Fig. 6b). Squares are related to the loading scheme 2, dots – to the scheme 5, triangles – to the scheme 4, dark rhombs – to the experimental data of Tennyson [2].

There is almost no difference in buckling loads between loading schemes for linear solutions. Nevertheless, the scheme 5 yields the lowest buckling loads. Buckling modes with cutouts are similar for all schemes.

Nonlinear solutions vary significantly for the studied schemes. Very small cutouts have a poor effect on buckling loads for different schemes because of relatively small deflections at limit load. But the influence of loading conditions is considerable for the cutouts $r > 4^o$. The scheme 4 turns out to yield the highest buckling load; the dependence in Fig. 5, b is non–monotonic. There is a slight increase of buckling load caused by constraint on shell deformation at $r \sim 6^o$.

3.3. *Thickness parameter influence*

In this investigation, we studied the effect of a circular cutout on buckling of compressed thin–walled cylinders using Lekkerkerker's parameter μ. The parameter is considered to be more reasonable [19] as it takes into account not only the cutout size, but also the shell thickness. To figure out its influence, additional series of numerical analyses have been performed for shells with $R/h = 500$ ($h = 0.28$ mm). The other geometrical characteristics remained unchanged.

Results of geometrically nonlinear analyses on Lekkerker's parameter μ for both R/h are shown in Tab. 1. Buckling loads of thicker shells are higher than those for shells with $R/h = 500$. The most significant difference is about 7%. It is observed for the shell with the largest cutout.

In Fig. 7, a we can see graphical dependences of buckling loads on parameter μ for two considered thicknesses. Black and white rhombs represent respectively limit and bifurcational loads for shells with $R/h = 500$. The description of other curves is presented above (Section 3.1 and Fig. 3). As it is expected, linear solutions coincide for shells with different R/h.

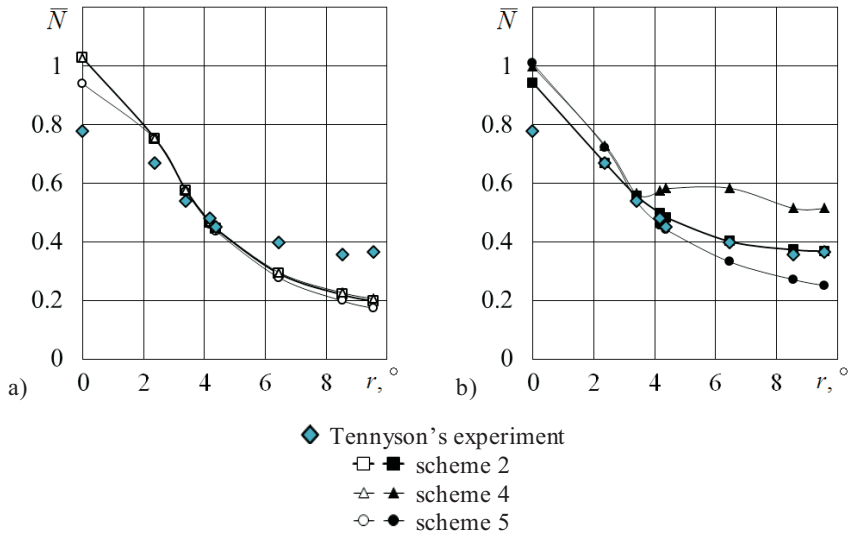

Figure 6 Dependences of relative experimental [2] and numerical critical (a) and limit (b) loads on cutout r for three different loading schemes

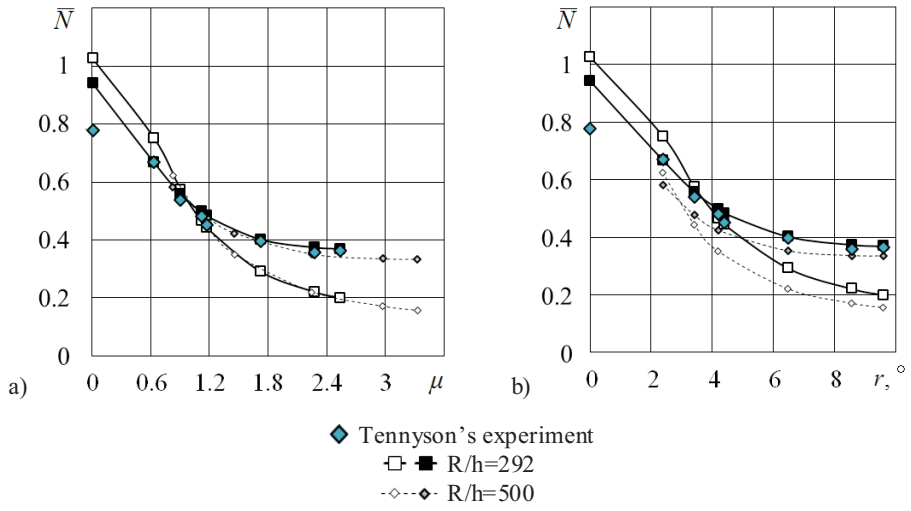

Figure 7 Dependences of relative experimental and numerical buckling loads on cutout r for the scheme 2

Table 1 Relative limit loads $\bar{N}$ for different parameters R/h and μ

	μ						
R/h		0.633	0.904	1.16	1.72	2.27	2.54
	292	0.668	0.558	0.484	0.402	0.374	0.369
	500	0.640	0.560	0.483	0.400	0.351	0.345

Fig. 7b illustrates the same results on angular size r of cutouts. For both types of analysis, buckling loads of thinner shells are lower; and increase of r leads to slight decrease of the difference between buckling loads for shells with different R/h in the studied range of cutouts.

4. Conclusions

The numerical research of buckling of axially compressed cylindrical shells with single circular cutouts is performed for the comparison with Tennyson's famous experiment. Linear and geometrically nonlinear analyses are realised in the environment of ANSYS program code for three different loading schemes. For all loading conditions, results of geometrically nonlinear calculations are higher than results of linear solution if $r \geq 4^o$.

An excellent agreement of numerical results (buckling loads and modes) with the experimental data is obtained in the geometrically nonlinear analyses by means of taking into account the particularities of shell loading. The loading scheme in the experiment represents non-classical axial compression realised by controlled displacements with possible free rigid elements at the shell edges.

The other two considered loading schemes provide upper and lower bounds for experimental data. These schemes are classical types of axial compression realised respectively with uniform displacements or uniform forces distributed along the shell edges.

Real buckling loads of axially compressed cylinders with single circular cutouts depend on the parameter μ which is proportional to cutout size divided by the square root of product of the shell radius and its thickness. This parameter catches the most significant dependence of buckling load on shell geometrical parameter. However, the calculations show that decrease of the shell thickness about two times leads to about 7% decrease of buckling load in the studied range of cutouts.

The performed comparison proves the efficiency of ANSYS software for a design of the shells with highly non-homogeneous stress strain state and significantly nonlinear deformation.

Acknowledgements

This work is supported by the Alexander von Humboldt Foundation (Institutional academic cooperation program, grant no. 3.4. – Fokoop. – UKR/1070297). Fruitful discussions with Dr. A. Evkin and his comments are also gratefully acknowledged.

References

[1] **Lur'e, A. I.**: Static of thin–walled elastic shells, AEC-tr-3798, Atomic Energy Commission, (translated from Moscow: *State Publishing House of Technical and Theoretical Literature*,) **1947**.

[2] **Tennyson, R. C.**: The effect of unreinforced circular cutouts on the buckling of circular cylindrical shells under axial compression, *Journal of Engineering for Industry*, 90(4), 541–546, **1968**.

[3] **Lykhachova, O. and Krasovsky, V.**: Numerical simulation of buckling tests of axially compressed cylindrical shells with one circular cutout (R. Tennyson's experiments), *Proc. Theoretical Foundations of Civil Engineering*, 22, WP, Warsaw, 133–136, **2014**.

[4] **Van Dyke, P.**: Stress about a circular hole in a cylindrical shell, *AIAA Journal*, 3, 1733–1742, **1965**.

[5] **Preobrazhenskii, I. N.**: Stability of thin–walled shells with holes (survey). Part 1, *Strength of Materials*, 14(1), 23–35, **1982**.

[6] **Preobrazhenskii, I. N.**: Stability of thin shells with cutouts (review). Part 2, *Strength of Materials*, 14(2), 218–225, **1982**.

[7] **Grigolyuk, E. I. and Fil'shinskii, L. A.**: Perforated plates and shells, *Nauka*, Moscow, (in Russian), **1970**.

[8] **Ashmarin, Y. A. and Guz, A. N.**: Stability of a shell weakened by holes (review), *Soviet Applied Mechanics*, **9**(4), (1973), 349-358, (translated from *Prikladnaya Mekhanika*, **9**(4), (1973), 3-15).

[9] **Simitses, G. J.**: Buckling and postbuckling of imperfect cylindrical shells. A review, *Applied Mechanics Review*, 39(10), 1517–1524, **1986**.

[10] **Teng, J. G.**: Buckling of thin shells. Recent advances and trends, *Applied Mechanics Review*, 49(4), 263–274, **1996**.

[11] **Song, C–Y.**: Buckling of cylindrical shells under non-uniform axial compressive stress, *Journal of Zhejang University*, 3(50), 520–531, **2002**.

[12] **Elishakoff, I.**: Resolution of the Twentieth Century Conundrum in Elastic Stability, 1^{st} ed., World Scientific Publishing Company, **2014**.

[13] **Obodan, N. I., Lebedev, O. G. and Gromov, V. A.**: Nonlinear behaviour and stability of thin–walled shells – Solid Mechanics and its applications, New York–London: *Springer Dordrecht Heidelberg*, 199, **2013**.

[14] **Kwok, R. M. K.**: *Mechanics of damaged thin–walled cylindrical shells*, Ph.D. Thesis, University of Surrey, Guildford, **1991**.

[15] **Dzyuba, A. P., Prokopalo, E. F. and Dzyuba, P. A.**: Bearing capacity of cylindrical shells with the perforations, *Lira*, Dnipropetrovsk, (in Ukrainian), **2014**.

[16] **Hilburger, M. W.**: Buckling and failure of compression-loaded composite laminated shells with cutouts, *AIAA Journal*, 21(99), 1–13, **2007**.

[17] **Hilburger, M. W. and Starnes, Jr. J. H.**: Effects of imperfections on the buckling response of compression–loaded composite shells, *Journal of Non–linear Mechanics*, 37, 623–643, **2002**.

[18] **Kriegesmann, B., Hilburger, M. W. and Rolfes, R.**: The effect of geometric and loading imperfections on the response and lower–bound buckling load of a compression–loaded cylindrical shell, *AIAA Journal*, 1–10, **2012**.

[19] **Starnes, Jr. J. H.**: Effect of a circular hole on the buckling of cylindrical shells loaded by axial compression, *AIAA Journal*, 10(11), 1466–1472, **1972**.

[20] **Jullien, J.-F. and Limam, A.**: Effect of openings on the buckling of cylindrical shells subjected to axial compression, *Thin–Walled Structures*, 31, 187–202, **1998**.

[21] **Lykhachova, O. V. and Schmidt, R.**: Deformation and buckling of axially compressed elastic cylindrical shells with transversal cut in experiments and numerical simulations, *Shell Structures: Theory and Applications*, **3**, Taylor & Francis Group, London, 219–222, **2014**.

[22] **Krasovsky, V. L., Lykhachova, O. V.**: Numerical buckling solutions of cylindrical shells with one transversal cut under different conditions of axial compression, *Proc. Stability of Structures*, 14, LP, Lodz, 61–62, **2015**.

[23] **ANSYS** Inc. Academic Research, Release 13.0, Help System, *Mechanical Analysis Guide.*